Journal of Applied Physics

# Modeling of yield estimation for DNA strand breaks based on Monte Carlo simulations of electron track structure in liquid water

Cite as: J. Appl. Phys. **126**, 124701 (2019); https://doi.org/10.1063/1.5115519
Submitted: 18 June 2019 . Accepted: 26 August 2019 . Published Online: 25 September 2019

Yusuke Matsuya, Takeshi Kai, Yuji Yoshii, Yoshie Yachi, Shingo Naijo, Hiroyuki Date, and Tatsuhiko Sato

Journal of Applied Physics ARTICLE scitation.org/journal/jap

# Modeling of yield estimation for DNA strand breaks based on Monte Carlo simulations of electron track structure in liquid water

Cite as: J. Appl. Phys. **126**, 124701 (2019); doi: 10.1063/1.5115519
Submitted: 18 June 2019 · Accepted: 26 August 2019 ·
Published Online: 25 September 2019



Yusuke Matsuya,[1,2,a)] Takeshi Kai,[1] Yuji Yoshii,[3] Yoshie Yachi,[4] Shingo Naijo,[4] Hiroyuki Date,[2] and Tatsuhiko Sato[1]

## AFFILIATIONS

[1]Nuclear Science and Engineering Center, Research Group for Radiation Transport Analysis, Japan Atomic Energy Agency (JAEA), 2-4 Shirakata, Tokai, Ibaraki 319-1195, Japan
[2]Faculty of Health Sciences, Hokkaido University, Kita-12 Nishi-8, Kita-ku, Sapporo, Hokkaido 060-0812, Japan
[3]Central Institute of Isotope Science, Hokkaido University, Kita-15 Nishi-7, Kita-ku, Sapporo, Hokkaido 060-0815, Japan
[4]Graduate School of Health Sciences, Hokkaido University, Kita-12 Nishi-8, Kita-ku, Sapporo, Hokkaido 060-0812, Japan

[a)]**Author to whom correspondence should be addressed:** matsuya.yusuke@jaea.go.jp

## ABSTRACT

DNA strand breaks are induced in cells mainly composed of liquid water along ionizing radiation tracks. For estimating DNA strand break yields, track structures for electrons in liquid water in Monte Carlo simulations are of great importance; however, detailed simulations to obtain both energy deposition and free radical reaction to DNA are time-consuming processes. Here, we present a simple model for estimating yields of single- and double-strand breaks (SSB, DSB, and DSB/SSB ratio) based only on spatial patterns of inelastic interactions (i.e., ionization and electronic excitation) generated by electrons, which are evaluated by the track structure mode of Particle and Heavy Ion Transport code System without analyzing the production and diffusion of free radicals. In the present model, the number of events per track and that of a pair composed of two events within 3.4 nm (10 base pairs) were stochastically sampled for calculating SSB and DSB yields. The results calculated by this model agree well with other simulations and experimental data on the DSB yield and the DSB/SSB ratio for monoenergetic electron irradiation. This model also demonstrates the relative biological effectiveness at the DSB endpoint for various photon irradiations, indicating that the spatial pattern composed of ionization and electronic excitation without physicochemical and chemical stages is sufficient to obtain the impact of electrons on the initial DNA strand break induction.



## I. INTRODUCTION

Biological effects after exposure to the ionizing radiation arise from initial damage to the DNA helix structure.[1] A variety of DNA lesions, including single- and double-strand breaks (SSBs and DSBs), are induced along the radiation track.[1–3] A Monte Carlo code for the track structure simulation at the nanometer scale in liquid water[4–6] is a powerful tool for the mechanistic investigation of the DNA damage induction.[7,8] Most of the energy deposition by the ionizing radiation is composed of secondary electrons,[5] thus a reliable code for predicting the track structure of electrons is required for computing the spatial distribution of DNA hits. However, radiation transport qualities in the low energy range below sub-kiloelectron volt remain uncertain.

Several codes for simulating electron tracks have been developed based on electron scattering cross sections in water vapor (i.e., PARTRAC[9] derived from MOCA-8[10] and KURBUC[11]) or on a combination of analytical and interpolated cross sections for liquid water (GEANT4-DNA[12]). In contrast, Particle and Heavy Ion Transport code System (PHITS),[13] which was developed based on the first-principles calculation, can simulate the track structure of electrons in liquid water in a wide incident energy range from 1 meV to 1 MeV.[14–19] The electron track structure mode (etsmode) has also been released publicly,[13] which enables the evaluation of the impacts of low energy electrons on the DNA strand break induction.

Among DNA strand breaks, DSBs are recognized as fatal lesions due to the complexity of the lesions and the difficulty of repair.[20,21]

For this reason, many researchers have investigated the DSB yield by means of Monte Carlo codes[3,7,22] and biological experiments.[2,23–26] To evaluate DNA strand break types, several trials for calculating physical, physicochemical, and chemical processes[3–5,7,9,22,27–29] have been performed. However, obtaining both the energy deposition and the radical reaction within a cylinder of DNA is a time-consuming process. In contrast, by focusing on the spatial analysis of density-based spatial clustering application with noise (DBSCAN),[22,30,31] we can evaluate the degree of aggregation (aggregation index) by inelastic interactions for every electron track.[22] Assuming that physicochemical and chemical stages end close to the inelastic events,[27] the spatial positions of the events and their pairs should enable us to stochastically predict SSB and DSB yields. Thus, our interest is directed to developing a simple model for estimating DNA strand break yields, without considering free radicals.

In this study, we present a simple model for estimating DNA strand breaks (SSB, DSB, and DSB/SSB ratio) based only on the physical processes of electrons. The track structure mode in the PHITS code, which was verified with other simulations and experimental data in this study, was used to obtain the spatial distribution of inelastic interactions. Through this estimation of DNA strand break yields, we show that the spatial pattern of inelastic interactions can be directly linked to the estimation of DNA damage yields.

## II. MATERIALS AND METHODS

### A. Physical processes in PHITS

PHITS version 3.10[13] adapting the electron track structure mode (etsmode) was used for simulating electron tracks. The physics processes were composed of elastic scattering, electron ionization, electronic excitation, dissociative electron attachment, vibrational excitation, rotational excitation, and photon excitation.[14–19] The information on inelastic interactions was output by the use of a tally named "t-interact." To reduce the computational time, the cut-off energy was set depending on the incident electron energy, $E_{in}$, i.e., 1 eV for $E_{in} > 2$ eV and 1 meV for $E_{in} \leq 2$ eV. We transported at least 1000 electrons for each electron kinetic energy to obtain calculation results. The reproducibility was checked by performing the calculation twice.

### B. Calculation of physical qualities

To validate the electron track structure in PHITS from the viewpoint of radiation physics, we calculated the range (i.e., path length and penetration), mass stopping power in MeV cm$^2$/g, and dose-mean lineal energy with the site diameter ranging from 2 nm (on the DNA scale) to 1 $\mu$m (on the chromosome scale).

As for the two types of ranges, path length means the total length of the path followed by the electron particle, while penetration rests on the radius vector between the starting point and the stopping point.[32] The stopping power is calculated following the report by Ashley[33] as reported previously.[14] The dose-mean lineal energy ($y_D$) was calculated according to ICRU report 36.[34] The lineal energy $y$ in keV/$\mu$m is given by

$$y = \frac{\varepsilon}{\bar{l}}, \tag{1}$$

where $\varepsilon$ is the energy deposited in the site and $\bar{l}$ is the mean chord length of the site which is defined as $\bar{l} = 4r_d/3$ ($r_d$ is the site radius in micrometers). Averaging the lineal energy from the viewpoint of the probability density of dose, $y_D$ in keV/$\mu$m is expressed as

$$y_D = \int y d(y) \mathrm{d}y, \tag{2}$$

where $d(y)$ is the probability density of dose in the site. For obtaining $d(y)$, we used the uniform sampling technique along each track, as reported previously.[35]

The calculated results were compared to ICRU reports[36,37] and published data containing experiments and the other simulation results.[38–42]

### C. Stochastic hit model for strand break induction

To calculate yields of SSBs and DSBs, we assumed that the DNA double helix is randomly placed along the electron track as shown in Fig. 1(a). DSBs are generally defined as the minimum of two strand breaks[4,43] within 10 base pairs (i.e., 3.4 nm).[44] Assuming that ionization and electronic excitation are potential causes to induce DNA strand breaks,[5,22] we scored the number of the events per track [Fig. 1(b)] and that of the event pair (so-called linkage) within 3.4 nm per track [Fig. 1(c)]. Assuming that the number of events per keV $N_{event}/E_{in}$ and that of linkage per keV $N_{link}/E_{in}$ are proportional to the induction yield of a SSB and a DSB, respectively, we defined $k_{SSB}$ and $k_{DSB}$ as proportion coefficients for SSB and DSB inductions (keV/Gy/Da), respectively. The yields of SSB $Y_{SSB}$ and DSB $Y_{DSB}$ (/Gy/Da) as a function of electron incident energy are given by

$$Y_{SSB}(E_{in}) = k_{SSB} \frac{N_{event}}{E_{in}}, \tag{3}$$

$$Y_{DSB}(E_{in}) = k_{DSB} \frac{N_{link}}{E_{in}}. \tag{4}$$

It should be noted that two SSBs within 3.4 nm is classified as a DSB,[44] so we subtracted the DSB yield from the SSB yield. These coefficients were found to reproduce the experimental yields of SSB and DSB after exposure to 220 kVp X-rays.[45,46] The yield for photon spectra is given as the averaged value expressed as

$$\overline{Y_*} = \int Y_* (E_{in}) f(E_{in}) \, \mathrm{d}E_{in}, \tag{5}$$

where $\overline{Y_*}$ is the average yield of strand breaks for cases of electron spectra (* represents either SSB or DSB), and $f(E_{in})$ is the probability density of electron spectra generated by the photon irradiation. To verify this model, the calculated DSB yields and DSB/SSB ratio as a function of electron kinetic energy were compared to other simulations by Friedland *et al.*[47] and available experimental data.[2,48–50]

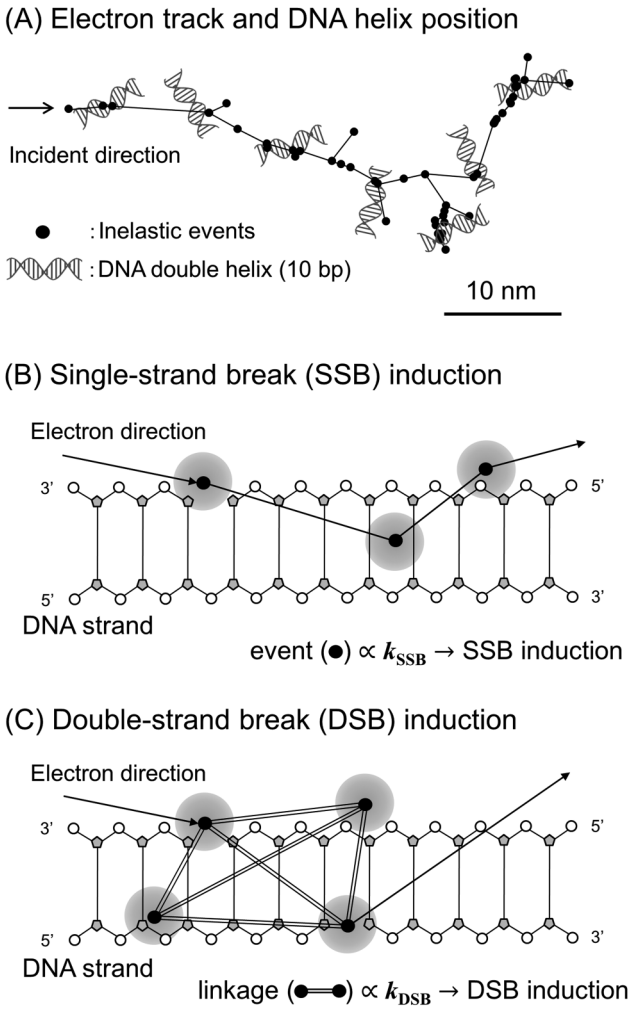


**FIG. 1.** Schematic representation of modeling of DNA strand break induction: (a) is the relation between the electron track structure and the DNA double helix in the present model, (b) is the single-hit model for SSB induction, and (c) is the double hits model for DSB induction. The DNA double helix is assumed to be randomly placed along the electron track [Fig. 1(a)]. The numbers of inelastic events and the linkages composed of two events within 3.4 nm (10 base pairs[44]) were scored. To calculate the yield of SSBs and DSBs, the proportionality constants for SSBs and DSBs are defined as $k_{SSB}$ and $k_{DSB}$, respectively.

### D. Experimental DSB detected by using γ-H2AX

To further validate the present DNA damage model, we collected experimental DSB data from the literature[26,35,49,51–55] and also performed a γ-H2AX focus formation assay. The experimental number of DSBs per nucleus was normalized to be the DSB-deduced relative biological effectiveness ($RBE_{DSB}$) to the standard radiation of 200 kVp X-rays.

In this *in vitro* experiment, normal human diploid lung fibroblast (WI-38) cell line (CCL-75, ATCC, Manassas, VA) and Chinese hamster lung fibroblast (V79-379A) cell line (IFO50082, JCRB Cell Bank, Japan) were used for additionally obtaining $RBE_{DSB}$. Following a previous report,[56] WI-38 cells were maintained in the cell culture medium [Dulbecco's modified Eagle's medium/Nutrient Mixture F-12 (DMEM/F12) (D8437, Sigma Life Science) supplemented with 10% fetal bovine serum (FBS, Equitech-Bio Inc.)]. V79-379A cells were maintained routinely in Dulbecco's modified Eagle's (D0819, Sigma Life Science) supplemented with 10% FBS and 1% penicillin/streptomycin (Sigma Life Science). These cells were cultured at 37 °C in humidified 95% air and 5% CO2. After exposing the cells in the confluent monolayer to various types of X-ray irradiation (i.e., 40 kVp, 60 kVp, 80 kVp, 100 kVp, 120 kVp, and 150 kVp) with 1.0 Gy, we performed a γ-H2AX focus formation assay, as reported previously.[35,51] The cells were fixed 30 min after irradiation to observe the initial DNA damage response.

### E. Estimation of RBE at DSB endpoints for photon irradiation

After obtaining the experimental $RBE_{DSB}$, we calculated the yield of the DSB induction for a variety of photon irradiations using PHITS ver. 3.10.[13] We divided the calculation into three steps: the first step is calculating the electron spectrum generated by the photon irradiation, the second step is simulating the electron track structure, and the third step is estimating the DSB yield by the DNA damage model.

For the photon procedure, the geometries considered in the PHITS code are the same as the experimental conditions for each photon irradiation.[35,49,51–55] The electron gamma shower (EGS)[57] mode was adapted into PHITS and 1 keV was set as the cut-off energy. In the same manner, as the case of monoenergetic electron irradiation, we used etsmode for calculating the electron tracks and scored the ionization and electronic excitation sites. Using the output data, we calculated the average yield of the DSB induction based on Eqs. (4) and (5).

The types of photon spectrum simulated in this study were $^{60}$Co γ-rays, 6 MV-linac X-rays (in- or out-of-field area), $^{137}$Cs γ-rays, conventional X-ray (200 kVp, 250 kVp X-rays), soft X-ray series (150 kVp, 120 kVp, 100 kVp, 80 kVp, 60 kVp, 40 kVp, and 29 kVp X-rays), and ultra-soft X-ray series ($Ti_K$, $Al_K$, $Cu_L$, and $C_K$). The DSB yield ratios of some photon irradiations and 200 kVp X-rays were calculated as the simulated $RBE_{DSB}$.

## III. RESULTS AND DISCUSSION

### A. Physical fundamental qualities of electrons

The range and the stopping power are shown in Figs. 2 and 3, respectively. As shown in Fig. 2, the calculated results were compared to ICRU report 37[37] in the high electron kinetic energy range and to experimental data reported by Konovalov *et al.*[38] in the low energy range. The Continuous Slowing Down Approximation (CSDA) range similar to the total path length coincides with ICRU report 37,[37] whilst the penetration by PHITS seems to reproduce the experimental data by Konovalov *et al.*[38]

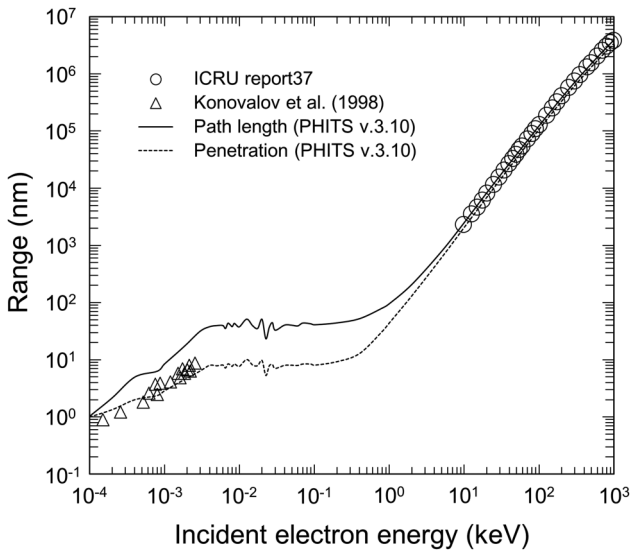


**FIG. 2.** Electron ranges calculated by the PHITS code. The path length (continuous slowing down approximation) and the penetration are evaluated as the electron range. The calculated ranges were compared to the data from ICRU 37[37] and by Konovalov *et al.*[38]

The energy loss rate per unit path length was also checked in comparison with published data,[36,37,39–41] as shown in Fig. 3. From these comparisons, it was verified that the etsmode can reproduce the published characteristics of electrons in a wide range of the incident energy.

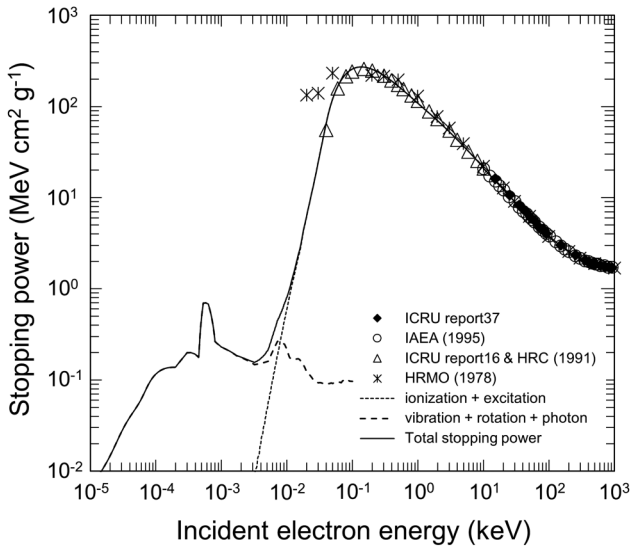


**FIG. 3.** Stopping power calculated by the PHITS code. Electron stopping power in liquid water calculated by using the PHITS etsmode is compared to the published data[39–41] and ICRU reports.[36,37]

Next, focusing on dosimetry on the nanometer scale, we calculated the dose-mean lineal energy $y_D$ in keV/$\mu$m and compared to other simulations by Geant4-DNA (adapting option 5).[42] Figure 4 shows the comparison between the PHITS calculation (present work) and Geant4-DNA data (option 5)[42] for 0.1, 0.5, and 1.0 keV monoenergetic electrons. Scaling down to 2 nm on the DNA scale from 1 $\mu$m on the chromosome scale, the $y_D$ value mostly increases, and the degree of the increment agreed well with the Geant4-DNA data.[42] We thus presumed that the electron track structure mode in PHITS is a reliable code for physically predicting the track structure of electrons.

### B. DNA damage yields for monoenergetic electrons

Based on the fundamental qualities of electrons (Figs. 2–4), we next estimated the DNA strand breaks (i.e., SSB and DSB) as a function of electron kinetic energy in kiloelectron volts. We present a simple stochastic model for calculating the DNA strand break yields (Fig. 1). The theory is based on hits to the DNA target packaged in the cell nucleus.

Figure 5 shows the calculated results of DNA strand break yields, where (a) is the DSB yield per Gy per dalton (Da) ($Y_{DSB}$), and (b) is the yield ratio of DSB and SSB ($Y_{DSB}/Y_{SSB}$). Considering the distance between two sites of inelastic interactions (ionization and electronic excitation) within 10 base pairs,[21] the track structure calculated by PHITS can demonstrate the peak of the DSB yield in the electron kinetic energy around 300 eV as shown in Fig. 5(a). By applying the model to the experimental yields of SSB and DSB after irradiation with 220 kVp X-rays, we obtained the coefficients $k_{SSB} = 5.66 \times 10^{-12}$

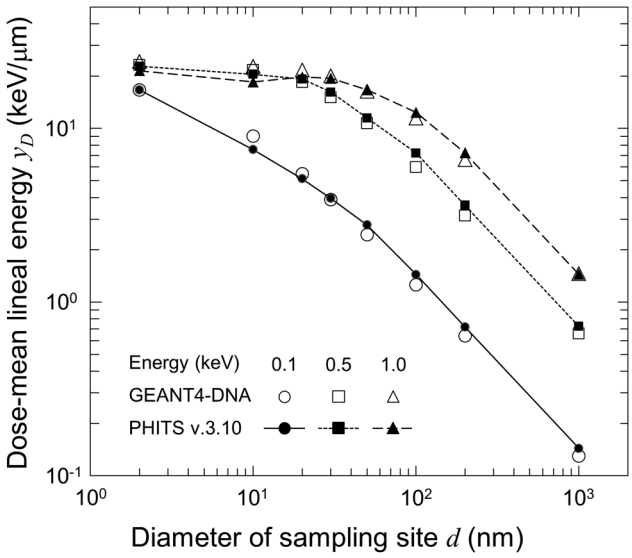


**FIG. 4.** Dose-mean lineal energy $y_D$ as a function of site diameter $d$ (nm). The $y_D$ values calculated by the PHITS code for 0.1, 0.5, and 1.0 keV monoenergetic electrons were compared with those by the GEANT4-DNA (option 5) calculation reported by Famulari *et al.*[42]

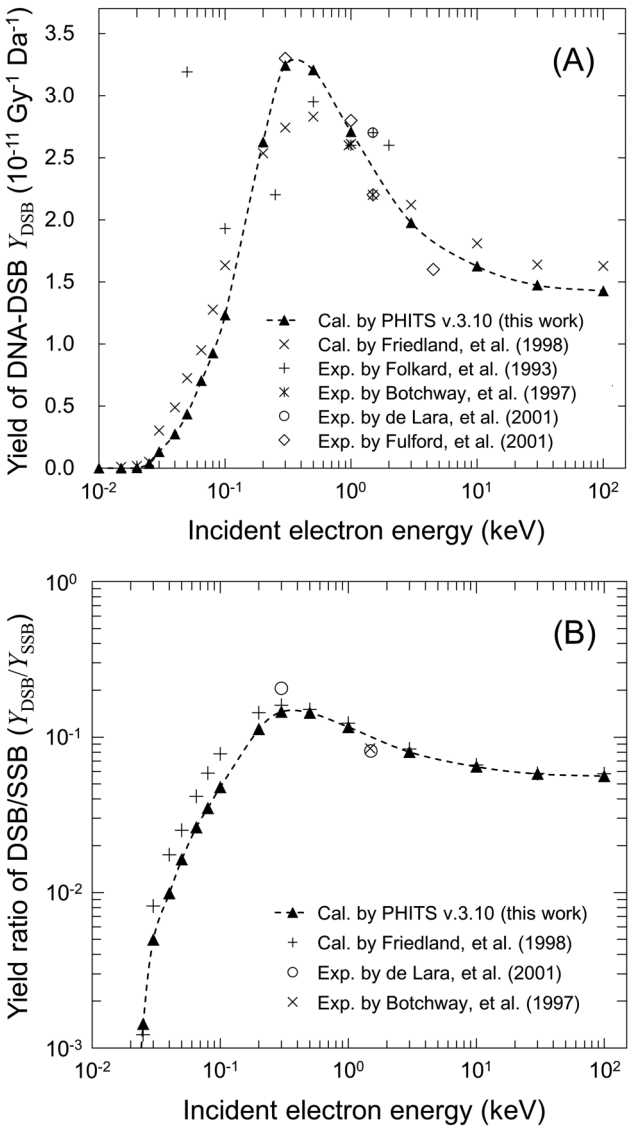


**FIG. 5.** Yield of DNA damage calculated by the PHITS code. (a) is the calculated yield of DNA-DSBs ($Y_{DSB}$) as a function of incident electron energy and (b) is the calculated yield ratio of DSB and SSB ($Y_{DSB}/Y_{SSB}$). The calculated yields were compared with other simulations by Friedland *et al.*[47] and several experimental data.[2,48–50]

(keV/Gy/Da) and $k_{DSB} = 1.61 \times 10^{-13}$ (keV/Gy/Da). These coefficients enable us to easily calculate DNA strand break sites from interaction sites according to a standard data format for the DNA damage (SDD format).[61] In comparison among the PHITS calculations, the other simulation results[47] and available experimental data[2,48–50] [Figs. 5(a) and 5(b)], this model exhibits good performance for reproducing the DSB yield ($Y_{DSB}$) and the ratio of DSB and SSB ($Y_{DSB}/Y_{SSB}$), suggesting that the spatial pattern of the two inelastic interactions (linkage) obtained by PHITS can be directly linked to yields of DNA strand breaks. However, it has been reported in recent decades that low energy electrons below 20 eV also have enough effect on inducing SSBs and DSBs.[58–60] Further model development is required in future studies.

Physicochemical and chemical stages were skipped in this study; however, we were successful in reproducing the DSB yield for monoenergetic electrons based only on physical processes. According to a previous report,[27] the maximum action distance of radical species (i.e., 0.0004 to 0.8120 nm) is much shorter than 10 base pairs (3.4 nm).[44] This implies that the spatial pattern of inelastic interactions is sufficient to estimate the yields of strand breaks. However, recombination of radical spices has to be considered for the case of higher linear energy transfer (LET) ionizing radiation (i.e., $^{12}C^{6+}$) more than electrons.[62] In this regard, it is also necessary to further develop this model so as to reproduce strand break yields for various LET irradiation.

### C. DSB yield for continuous energetic electrons generated by photons

We next tried to estimate the relative biological effectiveness (RBE) for a variety of photon irradiations. Concerning the model performance for the case of photons, we checked that the estimated yields of SSB and DSB for $^{60}$Co γ-rays [$Y_{SSB} = 28.3 \times 10^{-11}$ ($Gy^{-1}$ $Da^{-1}$) and $Y_{DSB} = 1.48 \times 10^{-11}$ ($Gy^{-1}$ $Da^{-1}$)] agreed with the experimental values ($29.0 \times 10^{-11}$ for SSB and $1.40 \times 10^{-11}$ for DSB).[49,50] After this one point verification, we compared the experimental $RBE_{DSB}$ (literature[26,35,51–55] and present work) with those calculated by PHITS for various photon irradiations.

The experimental mean number of nuclear DSBs increases as the mean photon energy becomes higher as listed in Table I. The simulation could reproduce this tendency by using a higher yield of DSBs for low energy electrons close to 300 eV [Fig. 5(a)]. Especially for the case of linac in-field irradiation, the dependency of the depth of $RBE_{DSB}$ could not be found from either the experiments or PHITS estimations. Meanwhile, the $RBE_{DSB}$ of the out-of-field linac X-rays was subtly higher than that of the in-field X-rays, which might be attributed to low energy scattered X-rays with relatively high $y_D$ values than in-field X-rays.[63] In addition, the $RBE_{DSB}$ values of the soft X-ray series (40–150 kVp) were relatively higher than conventional X-rays with 200 kVp because the soft X-rays generate lots of low energy electrons. This implies that diagnostic X-rays used in the medical field lead to higher biological impacts on DNA strand breaks induction than conventional and therapeutic X-rays.[35]

Based on the simulation results by PHITS (Figs. 2–5), it was suggested that the biological effects after exposure to electrons should be dependent on the kinetic energy as well as on the energy of secondary electrons generated by the photon irradiation. From these results (Table I), we concluded that the high frequency of double hits caused by lower energy electrons leads to a higher RBE even for the case of electron and photon irradiations.

**TABLE I.** RBE at the endpoint of DSB for various photon irradiations.

| Radiation type | Energy (calculation conditions) | $RBE_{DSB}$ Exp. | $RBE_{DSB}$ Cal. | Cell line type | Literature |
|---|---|---|---|---|---|
| $^{60}$Co γ-rays | 1.13 MeV, 1.33 MeV (6 mm depth) | 0.76 | 0.83 | CHO-K1, V79-4, HSF2 | Refs. 49, 53, and 55 |
| Linac X-rays in-field | 6 MV (1 cm depth at isocenter) | 0.73 | 0.83 | CHO-K1 | Ref. 35 |
| Linac X-rays in-field | 6 MV (3 cm depth at isocenter) | 0.74 | 0.84 | CHO-K1 | Ref. 35 |
| Linac X-rays in-field | 6 MV (5 cm depth at isocenter) | 0.76 | 0.84 | CHO-K1 | Ref. 35 |
| Linac X-rays in-field | 6 MV (10 cm depth at isocenter) | 0.85 | 0.83 | CHO-K1, WI-38 | Refs. 35, 51, and 52 |
| Linac X-rays out-of-field | 6 MV (10 cm depth, 10 cm from isocenter) | 0.86 | 0.96 | CHO-K1 | Ref. 3 |
| $^{137}$Cs-137 γ-rays | 662 keV (1 mm depth) | 0.92 | 0.89 | CHO-9 | Ref. 54 |
| Conventional X-rays | 250 kVp (No filtration, 1 mm depth) | 1.20 | 1.09 | CHO-K1 | Ref. 35 |
| Conventional X-rays | 200 kVp (1 mm depth) | 1.00 | 1.00 | CHO-K1 | Refs. 26, 35, and 51 |
| Soft X-rays | 150 kVp (1 mm depth) | 1.07 | 1.07 | WI-38, V79-379A | This work |
| Soft X-rays | 120 kVp (1 mm depth) | 1.09 | 1.07 | WI-38 | This work |
| Soft X-rays | 100 kVp (1 mm depth) | 1.13 | 1.10 | CHO-K1, WI-38, V79-379A | Ref. 35 and this work |
| Soft X-rays | 80 kVp (1 mm depth) | 1.10 | 1.06 | WI-38 | This work |
| Soft X-rays | 60 kVp (1 mm depth) | 1.16 | 1.11 | CHO-K1, WI-38, V79-379A | Ref. 35 and this work |
| Soft X-rays | 40 kVp (1 mm depth) | 1.18 | 1.03 | WI-38 | This work |
| Soft X-rays | 29 kVp (1 mm depth) | 0.87 | 0.95 | HSF2 | Ref. 55 |
| $Ti_K$ ultrasoft X-rays | 4.55 keV (surface) | 1.06 | 1.10 | V79-4 | Ref. 49 |
| $Al_K$ ultrasoft X-rays | 1.49 keV (surface) | 1.44 | 1.41 | V79-4 | Ref. 49 |
| $Cu_L$ ultrasoft X-rays | 0.96 keV (surface) | 1.75 | 1.62 | V79-4 | Ref. 49 |
| $C_K$ ultrasoft X-rays | 0.28 keV (surface) | 1.80 | 1.80 | V79-4, HSF2 | Refs. 49 and 55 |

## IV. CONCLUSION

This work found that the track structure code considered in PHITS ver. 3.10 enables us to provide precise electron features on the scale from a single track (micrometers) to DNA (nanometers). The calculated series of fundamental physical qualities of electrons (i.e., range, stopping power, and nanodosimetry) and yields of strand breaks (SSBs and DSBs) were compared to published data including ICRU reports, other simulation results, and experimental data. The coordinates of inelastic events such as ionization and electronic excitation are directly linked to the DNA strand break (i.e., SSB and DSB) yields, suggesting that calculating physical processes is sufficient to reproduce initial DNA damage responses for a variety of electron kinetic energies. The good agreement of the DSB yield calculated by PHITS with experimental DSB data for both electron and photon irradiations suggests that clusters of electron interactions represented as high frequent double hits by lower energy electrons lead to a higher $RBE_{DSB}$. This code for calculating DNA strand breaks after the electron irradiation will be implemented in the PHITS package in the future.

## ACKNOWLEDGMENTS

We would like to thank Dr. Kenneth L. Sutherland (Graduate School of Medicine, Hokkaido University, Sapporo, Japan) who kindly spared time for the English proofreading of the manuscript. This work was supported by the Japan Society for the Promotion of Science KAKENHI (Grant Nos. 17K07022 and 19K17215).

The authors declare that they have no conflict of interest.

## REFERENCES

[1]G. B. Wouters and A. C. Begg, "Irradiation-induced damage and the DNA damage response," in *Basic Clinical Radiobiology*, edited by M. Joiner and A. J. van der Kogel (Hodder Arnold, London, 2009), pp. 11–26.
[2]M. Folkard, K. M. Prise, B. Vojnovic, S. Davies, M. J. Roper, and B. D. Michael, "Measurement of DNA damage by electrons with energies between 25 and 4000 eV," Int. J. Radiat. Biol. **64**, 651–658 (1993).
[3]R. Watanabe, S. Rahmanian, and H. Nikjoo, "Spectrum of radiation-induced clustered non-DSB damage—A Monte Carlo track structure modeling and calculations," Radiat. Res. **183**, 525–540 (2015).
[4]H. Nikjoo, D. T. Goodhead, D. E. Charlton, and H. G. Paretzke, "Energy deposition in small cylindrical targets by monoenergetic electrons," Int. J. Radiat. Biol. **60**, 739–756 (1991).
[5]H. Date, Y. Yoshii, and K. L. Sutherland, "Nanometer site analysis of electron tracks and dose localization in bio-cells exposed to X-ray irradiation," Nucl. Instr. Methods Phys. Res. B **267**, 1135–1138 (2009).
[6]G. Bäckström, M. E. Galassi, N. Tilly, A. Ahnesjö, and J. M. Fernández-Varea, "Track structure of protons and other light ions in liquid water: Applications of the LIonTrack code at the nanometer scale," Med. Phys. **40**(6), 064101 (2013).
[7]H. Nikjoo, D. Emfietzoglou, T. Liamsuwan, R. Taleei, D. Liljequist, and S. Uehara, "Radiation track, DNA damage and response—A review," Rep. Prog. Phys. **79**, 116601 (2016).
[8]S. Incerti, I. Kyriakou, M. C. Bordage, S. Guatelli, V. Ivanchenko, and D. Emfietzoglou, "Track structure simulations of proximity functions in liquid water using the Geant4-DNA toolkit," J. Appl. Phys. **125**, 104301 (2019).
[9]W. Friedland, M. Dingfelder, P. Kundrát, and P. Jacob, "Track structures, DNA targets and radiation effects in the biophysical Monte Carlo simulation code PARTRAC," Mutat. Res. **711**, 28 (2011).
[10]H. G. Paretzke, "Radiation track structure theory," in *Kinetics of Nonhomogeneous Processes*, edited by G. R. Freeman (Wiley, New York, 1987), pp. 89–170.

[11]T. Liamsuwan, D. Emfietzoglou, S. Uehara, and H. Nikjoo, "Microdosimetry of low-energy electrons," Int. J. Radiat. Biol. **88**, 899 (2012).
[12]S. Incerti, G. Baldacchino, M. Bernal, R. Capra, C. Champion, Z. Francis, S. Guatelli, P. Guèye, A. Mantero, B. Mascialino, P. Moretto, P. Nieminen, A. Rosenfeld, C. Villagrasa, and C. Zacharatou, "The Geant4-DNA project," Int. J. Mod. Simul. Scien. Comput. **1**(02), 157–178 (2010).
[13]T. Sato, Y. Iwamoto, S. Hashimoto, T. Ogawa, T. Furuta, S. Abe, T. Kai, P.-E. Tsai, N. Matsuda, H. Iwase, N. Shigyo, L. Sihver, and K. Niita, "Features of particle and heavy Ion transport code system (PHITS) version 3.02," J. Nucl. Sci. Technol. **55**, 684–690 (2018).
[14]T. Kai, A. Yokoya, M. Ukai, and R. Watanabe, "Cross sections, stopping powers, and energy loss rates for rotational and phonon excitation processes in liquid water by electron impact," Radiat. Phys. Chem. **108**, 13–17 (2015).
[15]T. Kai, A. Yokoya, M. Ukai, K. Fujii, and R. Watanabe, "Dynamics of low energy electrons in liquid water with consideration of Coulomb interaction with positively charged water molecules induced by electron collision," Radiat. Phys. Chem. **104**, 16–22 (2014).
[16]T. Kai, A. Yokoya, M. Ukai, and R. Watanabe, "Deceleration processes of secondary electrons produced by a high-energy Auger electron in a biological context," Int. J. Radiat. Biol. **92**, 645–659 (2016).
[17]T. Kai, A. Yokoya, M. Ukai, K. Fujii, and R. Watanabe, "Thermal equilibrium and prehydration processes of electrons injected into liquid water calculated by dynamic Monte Carlo method," Radiat. Phys. Chem. **115**, 1–5 (2015).
[18]T. Kai, A. Yokoya, M. Ukai, K. Fujii, and R. Watanabe, "Dynamic behavior of secondary electrons in liquid water at the earliest stage upon irradiation: Implications for DNA damage localization mechanism," J. Phys. Chem. A **120**, 8228–8233 (2016).
[19]T. Kai, A. Yokoya, M. Ukai, K. Fujii, T. Toigawa, and R. Watanabe, "A significant role of non-thermal equilibrated electrons in the formation of deleterious complex DNA damage," Phys. Chem. Chem. Phys. **20**, 2838 (2018).
[20]R. Roots, T. C. Yang, and L. Craise, "Impaired repair capacity of DNA breaks induced in mammalian cellular DNA by accelerated heavy ions," Radiat. Res. **78**, 38–49 (1979).
[21]M. Frankenberg-Schwager and D. Frankenberg, "DNA double-strand breaks: Their repair and relationship to cell killing in yeast," Int. J. Radiat. Biol. **58**, 569–575 (1990).
[22]Y. Yoshii, K. Sasaki, Y. Matsuya, and H. Date, "Cluster analysis for the probability of DSB site induced by electron tracks," Nucl. Instr. Methods Phys. Res. B. **350**, 55–59 (2015).
[23]K. M. Prise, S. Davies, and B. D. Michael, "Evidence for induction of DNA double-strand breaks at paired radical sites," Radiat. Res. **134**(1), 102–106 (1993).
[24]E. Beyreuther, E. Lessmann, J. Pawelke, and S. Pieck, "DNA double-strand break signaling: X-ray energy dependence of residual co-localised foci of g-H2AX and 53BP1," Int. J. Radiat. Biol. **85**, 1042–1050 (2009).
[25]E. P. Rogakou, D. R. Pilch, A. H. Orr, V. S. Ivanova, and W. M. Bonner, "DNA double-stranded breaks induce histone H2AX phosphorylation on serine 139," J. Biol. Chem. **273**(10), 5858–5868 (1998).
[26]R. Mori, M. Matsuya, Y. Yoshii, and H. Date, "Estimation of the radiation-induced DNA double-strand breaks number by considering cell cycle and absorbed dose per cell nucleus," J. Radiat. Res. **59**(3), 253–260 (2018).
[27]H. Nikjoo, P. O'Neill, T. Goodhead, and M. Terrissol, "Computational modelling of low-energy electron-induced DNA damage by early physical and chemical events," Int. J. Radiat. Biol. **71**(5), 467–483 (1997).
[28]S. Uehara and H. Nikjoo, "Monte Carlo simulation of water radiolysis for low-energy charged particles," J. Radiat. Res. **47**, 69–81 (2006).
[29]M. S. Kreipl, W. Friedland, and H. G. Paretzke, "Time- and space-resolved Monte Carlo study of water radiolysis for photon, electron and ion irradiation," Radiat. Environ. Biophys. **48**, 11–20 (2009).
[30]M. Ester, H.-P. Kriegel, J. Sander, and X. Xu, "A density-based algorithm for discovering clusters in large spatial databases with noise," in *Proceeding of 2nd International Conference on Knowledge Discovery and Data Mining (KDD-96)* (AAAI Press, 1996), pp. 226–231.
[31]Z. Francis, C. Villagrasa, and I. Clairand, "Simulation of DNA damage clustering after proton irradiation using an adapted DBSCAN algorithm," Comput. Meth. Prog. Biol. **101**, 265–270 (2011).
[32]Z. Francis, S. Incerti, M. Karamitros, H. N. Tran, and C. Villagrasa, "Stopping power and ranges of electrons, protons and alpha particles in liquid water using the Geant4-DNA package," Nucl. Instr. Methods Phys. Res. B **269**, 2307–2311 (2011).
[33]J. C. Ashley, "Stopping power of liquid water for low-energy electrons," Radiat. Res. **89**(1), 25–31 (1982).
[34]ICRU Report 36, *International Commission on Radiation Units and Measurements* (ICRU, Bethesda, MD, 1983).
[35]Y. Yachi, Y. Yoshii, Y. Matsuya, R. Mori, J. Oikawa, and H. Date, "Track structure study for energy dependency of electrons and X-rays on the DNA double-strand breaks induction," Sci. Rep. (submitted).
[36]ICRU Report 16, *International Commission on Radiation Units and Measurements* (ICRU, Washington, DC, 1970).
[37]ICRU Report 37, *International Commission on Radiation Units and Measurements* (ICRU, Bethesda, MD, 1984).
[38]V. V. Konovalov, A. M. Raitsimring, and Y. D. Tsvetkov, "Thermalization lengths of "subexcitation electrons" in water determined by photoinjection from metals into electrolyte solutions," Radiat. Phys. Chem. **32**, 623–632 (1988).
[39]H. Paul and M. J. Berger, *Atomic and Molecular Data for Radiotherapy and Radiation Research, IAEA-ECDOC-799* (International Atomic Energy Agency, Vienna, 1995), pp. 415–545.
[40]Y. Tabata, Y. Ito, and S. Tagawa, *Handbook of Radiation Chemistry* (CRC Press, Boca Raton, FL, 1991).
[41]A. Brodsky, *Physical Science and Engineering Data, Handbook of Radiation Measurement and Protection* (CRC Press, West Palm Beach, FL, 1978).
[42]G. Famulari, P. Pater, and S. A. Enger, "Microdosimetry calculations for monoenergetic electrons using Geant4-DNA combined with a weighted track sampling algorithm," Phys. Med. Biol. **62**, 5495–5508 (2017).
[43]M. Hanai, K. Yazu, and R. Hieda, "On the experimental distinction between SSBs and DSBs in circular DNA," Int. J. Radiat. Biol. **73**(5), 475–479 (1998).
[44]Z. Nikitaki, V. Nikolov, I. V. Mavragani, E. Mladenov, A. Mangelis, D. A. Laskaratou, G. I. Fragkoulis, C. E. Hellweg, O. A. Martin, D. Emfietzoglou, V. I. Hatzi, G. I. Terzoudi, G. Iliakis, and A. G. Georgakilas, "Measurement of complex DNA damage induction and repair in human cellular systems after exposure to ionizing radiations of varying linear energy transfer (LET)," Free Radic. Res. **50**(S1), S64–S78 (2016).
[45]M. Lobrich, P. K. Cooper, and B. Rydberg, "Non-random distribution of DNA double-strand breaks induced by particle irradiation," Int. J. Radiat. Biol. **70**, 493–503 (1996).
[46]M. Ljungman, S. Nyberg, J. Nygren, M. Eriksson, and G. Ahnstrom, "DNA-bound proteins contribute much more than soluble intracellular compounds to the intrinsic protection against radiation-induced DNA strand breaks in human cells," Radiat. Res. **127**, 171–176 (1991).
[47]W. Friedland, P. Jacob, H. G. Paretzke, and T. Stork, "Monte Carlo simulation of the production of short DNA fragments by low-linear transfer radiation DNA model," Radiat. Res. **150**, 170–182 (1998).
[48]S. W. Botchway, D. L. Stevens, M. A. Hill, T. J. Jenner, and P. O'Neill, "Induction and rejoining of DNA double-strand breaks in Chinese hamster V79-4 cells irradiated with characteristic aluminium K and copper L ultrasoft x-rays," Radiat. Res. **148**, 317–324 (1997).
[49]C. M. de Lara, M. A. Hill, D. Papworth, and P. O'Neill, "Dependence of the yield of DNA double-strand breaks in Chinese hamster V79-4 cells on the photon energy of ultrasoft x rays," Radiat. Res. **155**, 440–448 (2001).
[50]J. Fulford, H. Nikjoo, D. T. Goodhead, and P. O'Neill, "Yields of SB and DSB induced in DNA by ALK ultrasoft x-rays and alpha-particles: Comparison of experimental and simulated yields," Int. J. Radiat. Biol. **77**, 1053–1066 (2001).
[51]Y. Matsuya, Y. Ohtsubo, K. Tsutsumi, K. Sasaki, R. Yamazaki, and H. Date, "Quantitative estimation of DNA damage by photon irradiation based on the microdosimetric-kinetic model," J. Radiat. Res. **55**, 484–493 (2014).

[52]Y. Matsuya, Y. Satou, N. Hamada, H. Date, M. Ishikawa, and T. Sato, "DNA damage induction during localized chronic exposure to an insoluble radioactive microparticle," Sci. Rep. **9**, 10365 (2019).
[53]Y. Kinashi, S. Takahashi, G. Kashino, R. Okayasu, S. Masunaga, M. Suzuki, and K. Ono, "DNA double-strand break induction in Ku80-deficient CHO cells following boron neutron capture reaction," Radiat. Oncol. **6**, 106 (2011).
[54]O. Staszewski, T. Nikolova, and B. Kaina, "Kinetics of (-H2AX focus formation upon treatment of cells with UV light and alkylating agents," Environ. Mol. Mutagen. **49**, 734–740 (2008).
[55]M. Kühne, G. Urban, D. Frankenberg, and M. Löbrich, "DNA double-strand break misrejoining after exposure of primary human fibroblasts to CK characteristic X rays, 29 kVp X rays and $^{60}$Co γ rays," Radiat. Res. **164**(5), 669–676 (2005).
[56]N. Hamada, "Ionizing radiation response of primary normal human lens epithelial cells," PLoS One **12**(7), e0181530 (2017).
[57]H. Hirayama, Y. Namito, A. F. Bielajew, S. J. Wilderman, and W. R. Nelson, The EGS5 code system. SLAC Report 730, prepared for the Department of Energy, USA (2005).
[58]B. Boudaïffa, P. Cloutier, D. Hunting, M. A. Huels, and L. Sanche, "Resonant formation of DNA strand breaks by Low-energy (3 to 20 eV) electrons," Science **287**(5458), 1658–1660 (2000).
[59]J. Simons, "How do low-energy (0.1–2 eV) electrons cause DNA-strand breaks?," Acc. Chem. Res. **39**, 772–779 (2006).
[60]F. Martin, P. D. Burrow, Z. Cai, P. Cloutier, D. Hunting, and L. Sanche, "DNA strand breaks induced by 0–4 eV electrons: The role of shape resonances," Phys. Rev. Lett. **93**, 068101 (2004).
[61]J. Schuemann, A. L. McNamara, J. W. Warmenhoven, N. T. Henthorn, K. J. Kirkby, M. J. Merchant, S. Ingram, H. Paganetti, K. D. Held, J. Ramos-Mendez, B. Faddegon, J. Perl, D. T. Goodhead, I. Plante, H. Rabus, H. Nettelbeck, W. Friedland, P. Kundrát, A. Ottolenghi, G. Baiocco, S. Barbieri, M. Dingfelder, S. Incerti, C. Villagrasa, M. Bueno, M. A. Bernal, S. Guatelli, D. Sakata, J. M. C. Brown, Z. Francis, I. Kyriakou, N. Lampe, F. Ballarini, M. P. Carante, M. Davídková, V. Stepan, X. Jia, F. A. Cucinotta, R. Schulte, R. D. Stewart, D. J. Carlson, S. Galer, Z. Kuncic, S. Lacombe, J. Milligan, S. H. Cho, G. Sawakuchi, T. Inaniwa, T. Sato, W. Li, A. V. Solov'yov, E. Surdutovich, M. Durante, K. M. Prise, and S. J. McMahon, "A new standard DNA damage (SDD) data format," Radiat. Res. **191**(1), 76–92 (2019).
[62]R. D. Stewart, V. K. Yu, A. G. Georgakilas, C. Koumenis, J. H. Park, and D. J. Carlson, "Effects of radiation quality and oxygen on clustered DNA lesions and cell death," Radiat Res. **176**, 587–602 (2011).
[63]H. Okamoto, T. Kohno, T. Kanai, Y. Kase, Y. Matsumoto, Y. Furusawa, Y. Fujit, H. Saitoh, and J. Itami, "Microdosimetric study on influence of low energy photons on relative biological effectiveness under therapeutic conditions using 6 MV linac," Med. Phys. **38**, 4714–4722 (2011).